Evaporation of an oscillating drop

Y. Hu*[1], S. Tonini[1], G.E. Cossali[1], B. Weigand[2], J. Reutzsch[2], M. Frey[2]

[1]Dipartimento di Ingegneria e Scienze Applicate, Università degli studi di Bergamo, Italy
[2]Institute of Aerospace Thermodynamics, University of Stuttgart, Germany
*Corresponding author: yueqiao.hu@unibg.it

Introduction

The study of droplet dynamics has a long history due to its wide application in different fields, such as spray coating, fire suppression, aero-engine, pharmacology, etc.[1]. Much work has been done in drop evaporation[7, 3] and oscillation[8, 4], respectively. However, in most scenarios, these both proceed simultaneously and have an effect on the other one. Until now, only few papers[5, 6] referred to the evaporation of an oscillating droplet. In the present work, we consider the evaporation of an oscillating droplet, releasing the assumption of quasi-steady heat and mass diffusion into the gas phase. The conservation equations were solved by numerical methods using an in-house code (FS3D). The distribution of vapour flux of a spheroidal droplet at the droplet surface under oscillating conditions is discussed and compared with the results of a droplet under quasi-steady conditions.

Numerical approach

We ran the simulations using an in-house code (FS3D), which was developed for DNS of incompressible multiphase flows with sharp interfaces between immiscible phases. FS3D solves the incompressible Navier-Stokes equations as well as the energy equation for the phase transition. The interface reconstruction is realized by VOF and PLIC methods. Without any turbulence model, FS3D is able to resolve the smallest temporal and spatial scales by DNS. However, it requires large computational efforts, which could be met by employing OpenMP as well as MPI[2].

Formulation of the problem

We consider a droplet oscillating in a gaseous environment. The computational domain is shown in Figure 1, a spheroidal water droplet of initial semi-axis $a_r = 0.5mm$, $a_z = 0.6mm$ oscillates and evaporates in the air, in the middle of the domain, which has the dimensions $2.8mm \times 2.8mm \times 2.8mm$ (grid resolution $128 \times 128 \times 128$). All boundaries have continuous conditions. The surface tension coefficient, liquid dynamic viscosity, and vapour-air diffusivity coefficient are set to $76.40mN/m$, $0.003Pa \cdot s$, and $28.45 \times 10^{-6} m^2/s$, respectively. The ambient pressure is set at $0.965 \times 10^5 Pa$. The initial air temperature is $351K$, while the drop temperature is $350.8K$. The small temperature difference is chosen to decrease the influence of the initial temperature difference on the vapour concentration distribution and the computational cost.

The ratio of evaporation time scale $t_{ev} \propto \frac{R_d^2}{D}$ and oscillation time scale $t_{osc} \propto \sqrt{\frac{\rho R_d^3}{\sigma}}$ is defined as the parameter $\phi = \frac{t_{ev}}{t_{osc}}$. For drop oscillations without evaporation, the parameter ϕ goes to infinite. For the evaporation of spheroidal droplets under a quasi-steady assumption, the parameter ϕ nears to be zero. In the present work of an evaporating and oscillating drop, the parameter ϕ is about 7. Thus the release of the quasi-steady assumption is expected to yield different results.

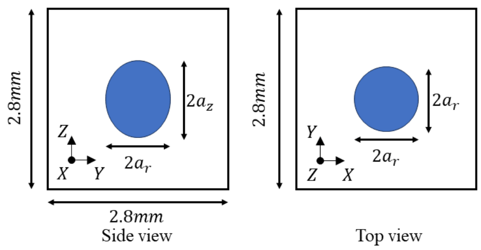

Figure 1. Computational domain of setup

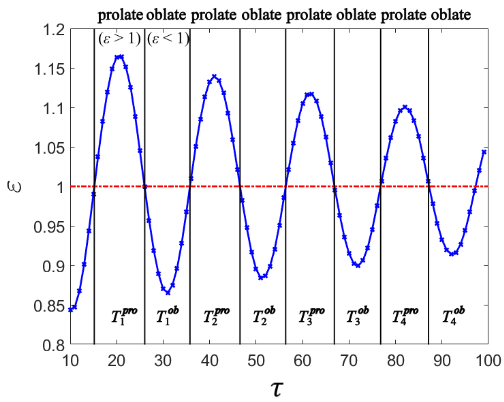

Figure 2. Aspect ratio with respect to time

Table 1. Time spent by droplet in the prolate and oblate shape.

	time in prolate shape (ms)	time in oblate shape (ms)	percentage of time in prolate shape (%)
period 1	T_1^{pro} : 1.641	T_1^{ob} : 1.531	51.73
period 2	T_2^{pro} : 1.605	T_2^{ob} : 1.572	50.52
period 3	T_3^{pro} : 1.588	T_3^{ob} : 1.561	50.43
period 4	T_4^{pro} : 1.576	T_4^{ob} : 1.544	50.51

Results and Discussion

In this section, the numerical results are presented and discussed. The decay of aspect ratio $\varepsilon = \frac{a_z}{a_r}$ is depicted in Figure 2, τ is defined as $\tau = \frac{\Delta t}{t}$ with $\Delta t = 0.154ms$. $\varepsilon > 1$ corresponds to a prolate shape, $\varepsilon < 1$ represents an oblate shape. Table 1 records the time spent by the droplet in the prolate or oblate shape in different periods. The time spent in prolate shape decreases with the period, the leap of time in oblate shape in the second period may be due to the initial instability. Figure 3 shows the velocity and temperature field in the XY and YZ plane at time $\tau = 44$ when the droplet has a prolate shape and ε is decreasing. No vortex flow inside the droplet is observed due to the small scale of the droplet. The temperature gradient across the interface is high due to the vaporization.

The spatial distribution of vapour flux of an oscillating droplet at the droplet surface shows different characteristics from that of a droplet under quasi-steady conditions. η is the cosine of the polar angle of an arbitrary position at the droplet surface, $\eta = 0$ represents the equator and $\eta = 1$ or -1 is the upper or lower pole. As shown in Figure 4 (a), the dimensionless vapour flux $\hat{\xi} = \frac{\xi}{\frac{\dot{m}_{ev}}{4\pi R_0^2}}$ in unsteady conditions reaches a higher value both at the equator and poles, regardless of the droplet shape. However, according to[9], the vapour flux ξ of a spheroidal droplet under quasi-steady conditions is expressed as $\xi = (R_0^2 K_G)^{1/4} \frac{\dot{m}_{ev}}{4\pi R_0^2}$. The dimensionless vapour flux $\hat{\xi}$ is proportional to the dimensionless Gauss curvature to the quarter power. Figure 4 (b) shows the distribution of the dimensionless vapour flux of a spheroidal droplet under quasi-steady conditions. It reaches a higher value at the equator for the oblate shape, while at the poles for the prolate shape.

By the way, the effect of diffusivity and viscosity is shown in Figure 5. Diffusivity in test 1, test 2, and test 3 are 28.45, 28.45, and $50 \times 10^{-6} m^2/s$, respectively. Viscosity in test 1, test 2, and test 3 are 0.003, 0.005, and 0.005 $Pa \cdot s$, respectively. The difference between test 2 and test 3 is negligible. The higher viscosity suppresses the oscillating amplitude, and the higher diffusivity has almost no effect.

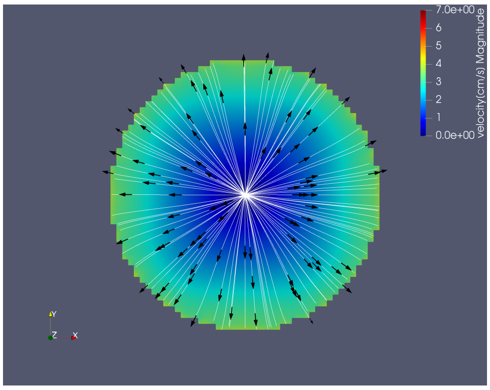

(a) Velocity field in XY plane

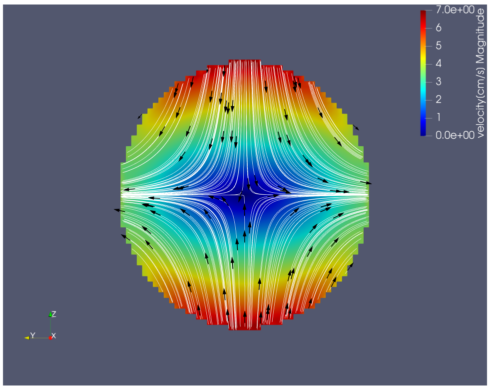

(b) Velocity field in YZ plane

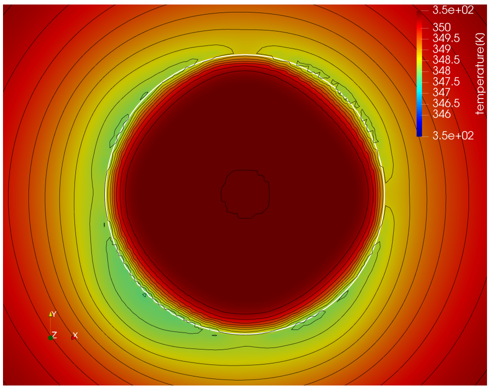

(c) Temperature field in XY plane

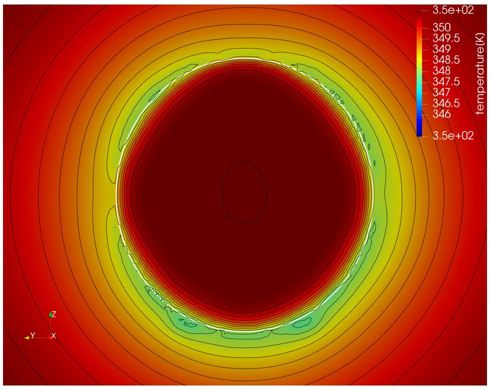

(d) Temperature field in YZ plane

Figure 3. Velocity and temperature field in the XY and YZ plane.

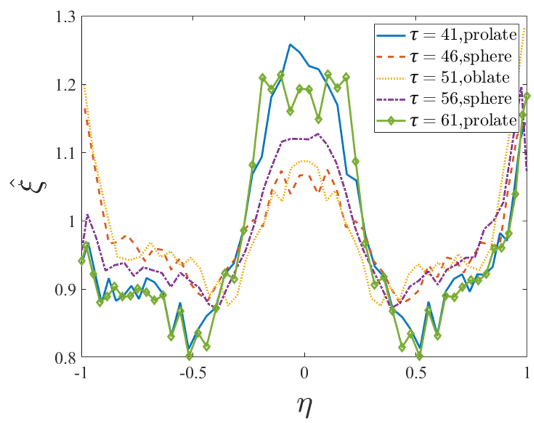

(a) Spatial distribution of vapour flux under unsteay conditions in one period, from simulation results($\phi = \dfrac{t_{ev}}{t_{osc}} \simeq 7$)

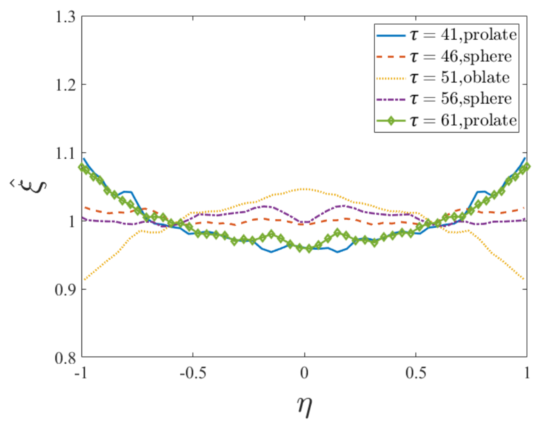

(b) Spatial distribution of vapour flux under quasi-steady conditions in one period, from theoretical results according to [9] ($\phi = \dfrac{t_{ev}}{t_{osc}}$ nears to be zero)

Figure 4. Comparison of spatial distribution of vapour flux under unsteady and quasi-steady conditions.

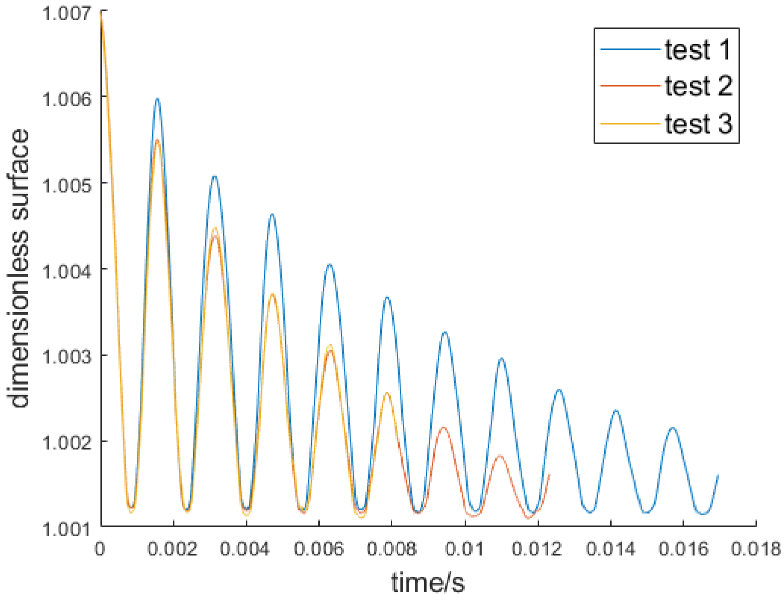

Figure 5. Effect of diffusivity and viscosity

Conclusion

An oscillating droplet under evaporating conditions is numerically investigated. The vapour flux of a droplet under unsteady conditions shows different characteristics from that of a droplet under quasi-steady conditions. It reaches a higher value at the equator and the poles at any moment, regardless of the droplet shape. The temperature has a high gradient across the interface due to the vaporization. The higher viscosity suppresses the oscillation amplitude, and the higher diffusivity has no effect. These findings urge a deeper analysis on the effect of taking into account the non-quasi steadiness on the modelling of evaporation of oscillating droplets.

References

[1] G. Brenn and S. Teichtmeister. Linear shape oscillations and polymeric time scales of viscoelastic drops. *Journal of fluid mechanics*, 733:504–527, 2013.

[2] K. Eisenschmidt, M. Ertl, H. Gomaa, C. Kieffer-Roth, C. Meister, P. Rauschenberger, M. Reitzle, K. Schlottke, and B. Weigand. Direct numerical simulations for multiphase flows: An overview of the multiphase code fs3d. *Applied Mathematics and Computation*, 272:508–517, 2016.

[3] N. A. Fuchs. *Evaporation and droplet growth in gaseous media*. Elsevier, 1959.

[4] H. Lamb. On the oscillations of a viscous spheroid. *Proceedings of the London Mathematical Society*, 1(1):51–70, 1881.

[5] F. Mashayek. Dynamics of evaporating drops. part i: formulation and evaporation model. *International journal of heat and mass transfer*, 44(8):1517–1526, 2001.

[6] F. Mashayek. Dynamics of evaporating drops. part ii: free oscillations. *International journal of heat and mass transfer*, 44(8):1527–1541, 2001.

[7] J. C. Maxwell. Diffusion. *Encyclopedia britannica*, 7(214):625–646, 1878.

[8] L. Rayleigh et al. On the capillary phenomena of jets. *Proc. R. Soc. London*, 29(196-199):71–97, 1879.

[9] S. Tonini and G. Cossali. An exact solution of the mass transport equations for spheroidal evaporating drops. *International Journal of Heat and Mass Transfer*, 60:236–240, 2013.